ing quantity is the magnitude of the cross section, since it determines whether the process is of practical interest at the presently available level of experimental precision. Unfortunately, in this calculation, as in most, the absolute magnitude of the cross sections is difficult to estimate reliably.

One might believe that our present assumptions are reasonable enough. Then the strong dependence of the cross section on incident energy indicates that at lower energies[10] (~40–50 MeV) the process ought to be within the purview of current experimental techniques. In particular, the region of large cross sections for the extremely asymmetric partition of energy among the breakup products appears to be encouraging for an experimental test.

---

†Work supported in part by the U. S. Atomic Energy Commission. A report of this work was submitted in partial fulfillment of the requirements for the degree of Ph.D. at the University of Maryland, College Park, in August, 1971. See Ref. 5, below.

*Present address: Department of Physics and Astronomy, University of Rochester, Rochester, New York 14627.

[1]W. Brandt and R. Laubert, Phys. Rev. Letters 24, 1037 (1970), and earlier references therein.

[2]H. Bando and A. Kuriyama, Progr. Theoret. Phys. (Kyoto) Suppl. 69 (1968); B. Gambhir and J. J. Griffin, Bull. Am. Phys. Soc. 15, 504 (1970).

[3]However, in the actual calculations the reduction of cross sections due to loss of flux to channels other than breakup is estimated by introducing an imaginary part in the optical potential representing $\overline{V}_n + \overline{V}_p$.

[4]K. R. Greider and L. R. Dodd, Phys. Rev. 146, 671 (1966).

[5]The relaxation of this condition is possible, but then one gets additional inhomogeneous terms in the subsequent integral equations. The generalized equations which do not require this condition are derived by B. L. Gambir, University of Maryland Technical Report No. 72-044, 1971 (to be published).

[6]B. L. Gambhir, see Ref. 5.

[7]Justification and range of validity of these approximations is discussed in some detail in Ref. 6 above.

[8]The choice of O^{16} as a target is governed by the enormous simplicity it provides for calculations. Target recoil, in this case, cannot be entirely neglected, but is expected to be not of serious consequence for the low-momentum-transfer region of the forward angles where the Pauli breakup cross sections are large.

[9]R. Serber, Phys. Rev. 72, 1008 (1947). Serber referred to the process described in this reference as deuteron stripping because of the manner in which he viewed it taking place.

[10]Calculated results for these low energies have not been reported because of the fact that our second assumption, $\Omega_i^\dagger |\phi_0 K_0\rangle = N |\phi_0 K_0^\dagger\rangle$, does not hold very well at these low energies. See Ref. 6.

PHYSICAL REVIEW C VOLUME 5, NUMBER 6 JUNE 1972

Electromagnetic Transitions from the Isobaric Analog States in ^{13}C, ^{19}F, and ^{31}P

M. R. Gunye and Chindhu S. Warke
Tata Institute of Fundamental Research, Bombay 5, India
(Received 20 December 1971)

The recent experimental data on the decay of isobaric analog states in ^{13}C, ^{19}F, and ^{31}P to their low-lying normal-parity states are analyzed. The calculations are carried out in the framework of the Hartree-Fock projection method by considering all the nucleons in the configuration space of the first four major oscillator shells and employing a realistic nucleon-nucleon interaction. It is found that the calculated energy spectrum of ^{19}F, static moments, and $\Delta T=0$ electromagnetic transition strengths in these nuclei agree very well with the experimental data. The $\Delta T=1$ $M1$ transition strengths and the corresponding ft values calculated from the projected wave functions are also in good agreement with the experimental observations. The agreement for the $\Delta T=1$ transitions between the present and the shell-model calculations is found to be nearly as good as that in the case of $\Delta T=0$ transitions.

1. INTRODUCTION

The discovery of isobaric analog resonances[1] in medium- and heavy-mass nuclei made it clear that isospin is a useful concept beyond light nuclei as well. The usefulness of the isospin quantum number (T) follows from the observed narrow widths (few keV) of the analog resonances and from their positions, which agree with the corresponding theoretical predictions.[2] It was also realized that the study of analog resonances provides an important tool for nuclear spectroscopy,[3,4] since some ana-

log states, which lie in the continuum, are more easily accessible than their parent states. One obtains information about the wave functions of the parent of the analog state and also about the final states to which the analog state decays. Spectroscopic factors for the parent analog state are obtained from cross sections for elastic and inelastic proton scattering through the isobaric resonances.

In this paper, we consider the electromagnetic transitions from the isobaric analog states in ^{13}C, ^{19}F, and ^{31}P to their low-lying normal-parity states. The choice of these nuclei stems from the following two facts: (i) the large amount of experimental data recently available, and (ii) the feasibility of calculations in a large model space employing the projected Hartree-Fock (HF) formalism. In the calculations reported here, we have considered all the nucleons in the configuration space of the first four major oscillator shells and use the realistic nucleon-nucleon (NN) interaction.[5] The HF projection method is found to be quite successful[6] in predicting the observed properties of the low-lying states of the nuclei in the mass region under consideration. The most creditable point of this approach lies in avoiding the extra parameters in the calculations to obtain reasonable agreement with the experimental results.

In the present investigations, we are mainly concerned with three aspects of the calculations regarding $\Delta T=1$ transitions. The main point of our study is to find out whether the HF projection method successfully predicts the observed analog-state transition strengths to the low-lying states of the same parity. In case it does, it would imply that the analog state, which lies quite high in the continuum, also has the intrinsic structure described by a single determinant of deformed HF orbitals. Since quite often analog states lie above the proton thresholds, there would be some isospin mixing in these states.[7] The low-lying bound states of nuclei are almost pure isospin states.[8] The isospin mixing in analog states may be important in isospin-forbidden decay, but it would not have an important effect on the allowed electromagnetic decay. This is so because of our expectation that the mixed states of lower isospin value will not have large transition strengths to low-lying states. In the HF wave functions for odd-A nuclei, however, there is a small spurious isospin impurity even though one uses isospin-conserving NN interactions. We have ignored its expected small effect on our results.

The second aspect of our investigation is to find out whether the HF projection method gives results very close to those predicted by the shell-model calculations. Such agreement is found[9] in the case of $\Delta T=0$ transitions between low-lying nuclear states. If the same is found in the case of $\Delta T=1$ transitions, it would imply that both parts of the projected wave function which are sensitive to $\Delta T=0$ and $\Delta T=1$ transitions agree quite well with the corresponding parts of the shell-model wave function. The $\Delta T=0$ transitions in conjunction with the $\Delta T=1$ transitions would provide an accurate test for the theoretical description of the nuclear wave functions.

The third and the last part of the present work consists of calculating the allowed $\Delta T=1$ Gamow-Teller (GT) β-decay matrix elements between the parent of the analog state and the low-lying states of these nuclei. It is known[10] that if the contribution of the orbital part of the $M1$ operator is negligible compared to that of the isovector spin part, one gets an explicit relation between this ft value (of a $\Delta T=1$ GT transition) and the $M1$ transition strength from the analog state to the same low-lying states. We find, however, that the contribution from the orbital part of the $M1$ operator is not always negligible.

In Sec. 2, we present the theoretical expressions for the $\Delta T=1$ transition matrix elements derived from the HF projection method. In Sec. 3, this formulation is applied to study the electromagnetic transitions in ^{13}C, ^{19}F, and ^{31}P and β transitions from the parent of their analog states. The results of our calculations are compared with the experimental data and with the shell-model predictions in the same section. The conclusions are presented in Sec. 4.

2. $\Delta T=1$ TRANSITION MATRIX ELEMENTS

The details of the HF projection method with its application to calculate the nuclear spectra and the $\Delta T=0$ electromagnetic transition matrix element are given in our earlier work.[11] The results of Ref. 11 are used to calculate the low-lying nuclear states of ^{19}F and the $\Delta T=0$ electromagnetic transitions in all three nuclei under consideration. We present here only the derivation of $\Delta T=1$ transition matrix elements. The experimental analysis of the isobaric analog resonances observed in (p,p), (p,p'), and (p,n) reactions indicates the almost pure isospin character of the isobaric analog states (IAS). The small isospin mixing in IAS will not have any important effect on the allowed $\Delta T=1$ electromagnetic transitions. Neglecting the small spurious isospin impurity in the intrinsic HF state of odd-A nuclei, the wave function $\Psi^{J,T+1}_{M,T}(Z,N)$ for IAS is obtained by applying the isospin lowering operator T^- to the wave function $\Psi^{J,T+1}_{M,T+1}(Z-1,N+1)$ of the parent analog

state (PAS),

$$\Psi^{J,T+1}_{M,T}(Z,N)=[2(T+1)]^{-1/2}T^{-}\Psi^{J,T+1}_{M,T+1}(Z-1,N+1), \tag{1}$$

where the isospin T of the low-lying states of a nucleus with Z protons and N neutrons is $T=\frac{1}{2}(N-Z)$. The wave functions on the left and on the right side of Eq. (1) are obtained from the intrinsic HF states $\Phi_{K_f}(Z,N)$ and $\Phi_{K_i}(Z-1,N+1)$, respectively, by the projection method.[11,12] Here K_i (K_f) is the band quantum number of the initial (final) axial HF state. It is convenient to express the electromagnetic transition operator in the isospin formalism as

$$O=\tfrac{1}{2}\sum_{k=1}^{A}(O_n^k+O_p^k)+\sum_{k=1}^{A}(O_n^k-O_p^k)\,t_z^k. \tag{2}$$

In Eq. (2), O_n^k (O_p^k) is the neutron (proton) transition operator and t_z^k is the z component of the nucleon isospin operator $\vec{t}$. The $\Delta T=1$ transition matrix element of the operator O in Eq. (2) between the initial IAS in Eq. (1), $\Psi^{J_i,T+1}_{M_i,T}(Z,N)$, and the final state, $\Psi^{J_f,T}_{M_f,T}(Z,N)$, is given by

$$\langle\Psi^{J_f,T}_{M_f,T}(Z,N)|O|\Psi^{J_i,T+1}_{M_i,T}(Z,N)\rangle=[2(T+1)]^{-1/2}\left\langle\Psi^{J_f,T}_{M_f,T}(Z,N)\left|\sum_{k=1}^{A}(O_p^k-O_n^k)\,t_-^k\right|\Psi^{J_i,T+1}_{M_i,T+1}(Z-1,N+1)\right\rangle. \tag{3}$$

Using similar algebra as in Ref. 11, the matrix element on the right-hand side of Eq. (3) can be expressed in the form

$$(p^{J_i}_{K_iK_i}p^{J_f}_{K_fK_f})^{-1/2}(J_iM_i,\lambda\mu|J_fM_f)\sum_{\nu}(J_iK_f-\nu,\lambda\mu|J_fK_f)\left\langle\Phi_{K_f}(Z,N)\left|\sum_{k=1}^{A}O^k(\lambda\nu)\,t_-^k\,P^{J_i}_{K_f-\nu,K_i}\right|\Phi_{K_i}(Z-1,N+1)\right\rangle. \tag{4}$$

In Eq. (4), λ and ν are the rank and the component of the tensor operator $O_p^k-O_n^k$; $(J_1M_1,J_2M_2|J_3M_3)$ is the standard vector-coupling coefficient. The explicit expression for the overlap integral p^J_{KK} of the projection operator P^J_{KK} is evaluated in Ref. 11. The matrix element in expression (4) can further be simplified to

$$(J+\tfrac{1}{2})\int d\theta\sin\theta\,d^{J_i}_{K_f-\nu,K_i}(\theta)\left\langle\Phi_{K_f}(Z,N)\left|\sum_{k=1}^{A}O^k(\lambda\nu)\,t_-^k\,e^{-i\theta J_y}\right|\Phi_{K_i}(Z-1,N+1)\right\rangle, \tag{5}$$

where the functions $d^J_{MK}(\theta)$ are as those given by Rose.[13] It is straightforward algebra to show that

$$\left\langle\Phi_{K_f}(Z,N)\left|\sum_{k=1}^{A}O^k(\lambda\nu)\,t_-^k\,e^{-i\theta J_y}\right|\Phi_{K_i}(Z-1,N+1)\right\rangle=\sum_{p=1}^{Z}\sum_{n=1}^{N+1}(-)^{p+n}D_p^{Z-1}(\theta)\,D_n^N(\theta)\times\sum_{\alpha\beta m}(\alpha m_p|O^k(\lambda\nu)|\beta m)C^p_\alpha(K_f)C^n_\beta(K_i)d^j_{mm_n}(\theta). \tag{6}$$

Here $C^{p\,(n)}_{\alpha}(K)$ is the single-particle proton (neutron) wave-function expansion coefficient in the intrinsic HF state with band quantum number K. The klth element in the determinants $D_p^{Z-1}(\theta)$ of order $Z-1$ and $D_n^N(\theta)$ of order N are, respectively, given by

$$a^p_{kl}(\theta)=\sum_\alpha C^k_\alpha(K_f)C^l_\alpha(K_i)d^{j\,\alpha}_{m_km_l}(\theta),\quad k\neq p; \tag{7}$$

$$a^n_{kl}(\theta)=\sum_\alpha C^k_\alpha(K_f)C^l_\alpha(K_i)d^{j\,\alpha}_{m_km_l}(\theta),\quad l\neq n. \tag{8}$$

In the case of the $M1$ transition operator, the spin part of the matrix element in Eq. (3) is proportional to the corresponding GT β-decay matrix element. Using this fact, one obtains the known[10] relation between the ft value and the transition strength $B(M1,\sigma)$ arising from only the spin part of the $M1$ operator:

$$ft=\frac{11\,825}{(T+1)\,B(M1,\sigma)}. \tag{9}$$

In computing ft values we have employed Eq. (1) of Gunye and Warke.[14]

3. CALCULATIONS AND RESULTS

It is well known that the shell-model (SM) calculations for many-nucleon systems in a large configuration space are prohibitively complicated. In such a situation the next best thing that can be done is to employ the approximate variational wave functions obtained from the intrinsic HF state by the projection technique.[12] The results of this HF projection method for low-lying nuclear states are found[9] to be in good agreement with the corresponding SM results for few-nucleon systems in a small configuration space. In the calculations reported here, the realistic NN interaction of Elliott *et al.*[5] has been used and all the nucleons are explicitly considered in the configuration space of the first four major oscillator shells in HF calculations for the odd-A nu-

clei. This *NN* interaction is found to yield[6] quite satisfactory results for the low-lying nuclear states of *p*- and *sd*-shell nuclei. In all the nuclei under investigation here, the low-lying states are obtained from the lowest axially symmetric intrinsic HF states by the projection method.[12]

The computed energy spectrum of ^{19}F from the lowest $K=\frac{1}{2}$ intrinsic HF state is shown in Fig. 1 and is in fair agreement with the experimental spectrum. It should be stated here that the small values of the overlap integrals for the $J=\frac{7}{2}$, $\frac{11}{2}$, and $\frac{13}{2}$ states make the energy evaluation of these states rather inaccurate compared to that of lower states. It is gratifying to note that the present spectrum is in good agreement with the SM spectrum[15] obtained by considering only the valence nucleons in a truncated *sd*-shell model space. The SM calculation[15] employs the renormalized effective *NN* interaction, whereas we have used the Elliott *NN* interaction.[5] The good agreement between the two results shows that the renormalization effects are approximately incorporated by treating all nucleons in a large configuration space. By using the best-fit phenomenological effective interaction in the *sd*-shell SM calculation, Arima *et al.*[16] obtain comparatively much better agreement with the experimental spectrum except for their inverted sequence of $\frac{13}{2}^+$ and $\frac{7}{2}^+$, which did not happen in both the present and the earlier SM calculation.[15] The energy spectrum in the case of ^{13}C is found to be rather compressed as compared to the experimental one. This is expected from the fact that the energy spectrum of ^{12}C also turns out to be compressed[17] in the HF projection method using realistic *NN* interactions. The ^{31}P energy spectrum is not computed because of the obvious reason of labor and computer time involved in such a calculation.

The evaluation of the static moments and the matrix elements of β and γ transitions provides a good criterion to test the validity of the model wave functions. Our calculated values of the magnetic and quadrupole moments displayed in Table I compare very well with the experimental values wherever available. The present values of the static moments are also very close to the corresponding SM predictions.[16,18] The SM calculations[16,18] employ effective charges $e_p=1.5e$ and $e_n=0.5e$. Since our model space and active nucleons are quite large as compared to those in the SM calculations, we expect an effective charge smaller than $0.5e$. The results shown in all the tables in this paper are obtained with an effective charge of $0.2e$ in the case of $A=19$ and $A=31$ nuclei, whereas in the case of $A=13$ nuclei, the effective charge used is only $0.1e$. This smaller effective charge in *p*-shell nuclei can be understood from the fact that the excitation configuration space for *p*-shell nuclei is much larger than that for *sd*-shell nuclei.

The calculated $\Delta T=0$ electromagnetic transition strengths presented in Table II are in good agreement with the corresponding experimental data in the case of ^{13}C,[3,19] ^{19}O, and ^{19}F,[20] whereas the agreement in the case of ^{31}P (Ref. 4) is not so good. A similar trend is observed (Table II) in the agreement between the present and SM calculations[4,16,21] except for a few cases in $A=19$ nuclei. In the *E*2 transitions $\frac{11}{2}^+ \rightarrow \frac{9}{2}^+$ and $\frac{11}{2}^+ \rightarrow \frac{13}{2}^+$ in ^{19}F where a large discrepancy exists between the present and the SM results, there are also large uncertainties in the experimental values.[20] These *E*2 transitions therefore can not be taken as a test for discriminating between the two sets of calculations. It is unfortunate that the two calculations for the corresponding *M*1 transitions also do not give any preference for a particular model, since in the $\frac{11}{2}^+ \rightarrow \frac{13}{2}^+$ transition, the present result is closer to the experimental value, while in the $\frac{11}{2}^+ \rightarrow \frac{9}{2}^+$ transition, the SM result[16] agrees with the experimental one. Our calculated $\frac{3}{2}^+ \rightarrow \frac{5}{2}^+$ *M*1 transition strength in ^{19}O is definitely in very good

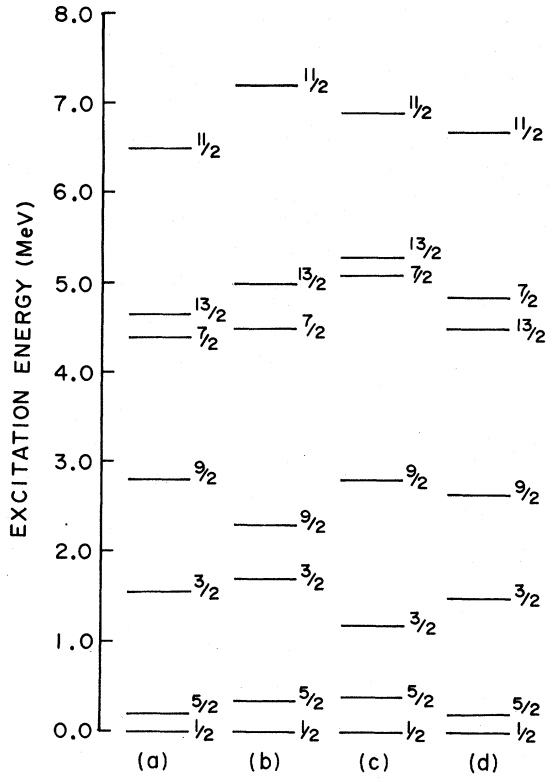

FIG. 1. Energy spectrum of ^{19}F: (a) Experimental spectrum, (b) the spectrum obtained in present calculations, (c) the shell-model spectrum of Ref. 15, (d) the shell-model spectrum of Ref. 16.

agreement with the precisely known experimental value. For this transition, the SM value quoted in Ref. 16 is too small as compared to our value, while that of Arima *et al.*[16] is large by nearly a factor of 2. In the case of ^{31}P, our computed strengths for $E2$ transitions are in better agreement with the experimental data[4] than those for the corresponding $M1$ transitions. The present $M1$ transition strengths are consistently larger than the experimental values. In the $\frac{7}{2}^+ \rightarrow \frac{5}{2}^+$ $M1$ transition, however, the SM value[4,21] is even larger than the present one. We wish to point out here that with zero effective charge the calculated $E2$ transitions are slower, while with the free-nucleon g factors the calculated $M1$ transitions are faster than the corresponding experimental transition rates. The reasonable agreement for the SM results (Table II) is obtained only after assigning[4,21] effective charges $e_p - e_n = e$ and $e_p + e_n = 2e(1.35 + 0.37E_x)$, where E_x is the average excitation energy, whereas we have consistently used $e_p = 1.2e$ and $e_n = 0.2e$. The computed strong $M1$ transition strength can be slowed down by quenching[4,21] of the g factors. The $M1$ transition strengths (Table II) are obtained by employing a quenching factor of 0.41 for the isovector $M1$ operator; the corresponding quenching factor in SM calculations[4,21] is 0.63. The same quenching factor (0.41) is employed in all the calculations in ^{31}P.

In the case of ^{13}C, the calculated $M1$ transition strengths and logft values for $\Delta T = 1$ transitions, as shown in Table III, are in very good agreement with the experimental data[3,19] and the SM results.[3,18] As pointed out by Polletti, Warburton, and Kurath,[22] the necessary condition for the validity of the model is for it to give the correct sign of the $E2/M1$ amplitude ratio in addition to its correct magntiude. The SM value of the $E2/M1$ ratio for the $\frac{3}{2}^-$ ($T = \frac{3}{2}$) to $\frac{1}{2}^-$ ($T = \frac{1}{2}$) transition is -0.167 by Kurath, as quoted in Ref. 3. Our value for this ratio is -0.157, as compared with the experimental value $-(0.095 \pm 0.07)$. In the case of ^{19}F, our results for the $M1$ decay of the IAS $\frac{5}{2}^+$ to the lowest $\frac{3}{2}^+$ and $\frac{5}{2}^+$ states are in good agreement with the experimental values.[20] The disagreement in the case of the decay to the $\frac{7}{2}^+$ state may be due to the inaccuracy in the wave function of this state in the projection method, as remarked earlier in the discussion of the energy spectrum of ^{19}F. The present results for the $M1$ decay of the excited IAS $\frac{3}{2}^+$ to the lowest $\frac{1}{2}^+$, $\frac{3}{2}^+$, and $\frac{5}{2}^+$ states are large by a factor of 2 to 4, as compared to the experimental values.[20] It is surprising, however, that the SM results quoted in Ref. 20 explain the decay of the excited IAS $\frac{3}{2}^+$ much better than the decay of the lowest IAS $\frac{5}{2}^+$. The results of the recent SM calculations of Arima *et al.*[16] for the decay of the IAS $\frac{5}{2}^+$ are similar to ours except for the decay to the $\frac{7}{2}^+$ state. They obtain[16] a value for this $M1$ decay strength very close to the large experimental value.[20] It is difficult to understand this large $M1$ strength of Ref. 16 in view of the fact that their other $M1$ transition strengths and all the logft values are close to ours. This large value may be due to the use of two different sets of potential parameters in the ^{19}O and ^{19}F SM calculations.[16] However, with this set of potentials, they fail to reproduce the $\Delta T = 0$ $\frac{3}{2}^+ \rightarrow \frac{5}{2}^+$ $M1$ transition strength in ^{19}O (Table II). Besides, the $\Delta T = 1$ $M1$ transition strengths from the excited IAS $\frac{3}{2}^+$ to the low-lying states of ^{19}F

TABLE I. The static magnetic dipole moment μ (in units of μ_N) and the electric quadrupole moment Q (in e fm^2) are tabulated. The experimental values along with those obtained from our present calculations and shell-model calculations are tabulated under the columns Expt, Present, and SM, respectively. In the case of ^{19}O and ^{19}F, the results of Arima *et al.* are shown in parentheses under the column SM.

Nucleus	Spin J	μ Expt	μ Present	μ SM	Q Expt	Q Present	Q SM
^{13}B	$\frac{3}{2}^-$		2.48			3.5	
^{13}C	$\frac{1}{2}^-$	0.70	0.84	0.70		0	
^{13}N	$\frac{1}{2}^-$	±0.32	−0.40			0	
^{19}O	$\frac{5}{2}^+$		−1.11	··· (−1.57)		−0.50	−0.10 (−0.12)
	$\frac{3}{2}^+$		−0.73	··· (−0.78)		2.10	2.90 (3.00)
^{19}F	$\frac{5}{2}^+$	3.69 ± 0.04	3.66	3.55 (3.71)	±11.0 ± 2.0	−9.00	−9.20 (−9.61)
	$\frac{1}{2}^+$	2.63 ± 0.01	2.87	2.87 (2.92)			
^{31}Si	$\frac{1}{2}^+$		−1.48				
^{31}P	$\frac{1}{2}^+$	1.13	0.81				

TABLE II. The $\Delta T=0$ electromagnetic transition strengths (in Weisskopf units) between the initial state (spin J_i) and final state (spin J_f) of the nuclei are displayed. Other notation is the same as in Table I.

			$E2$			$M1$		
Nucleus	J^π_i	J^π_f	Expt	Present	SM	Expt	Present	SM
^{13}C	$\frac{5}{2}^-$	$\frac{1}{2}^-$	3.18	4.50				
	$\frac{3}{2}^-$	$\frac{1}{2}^-$	>3.18	3.98		>0.025	0.63	0.67
^{19}O	$\frac{3}{2}^+$	$\frac{5}{2}^+$				0.018	0.020	<0.006 (0.036)
^{19}F	$\frac{3}{2}^+$	$\frac{1}{2}^+$	6.80 ± 0.70	7.15	6.31 (6.44)			
	$\frac{5}{2}^+$	$\frac{1}{2}^+$	6.87 ± 0.13	6.45	6.31 (6.51)			
	$\frac{9}{2}^+$	$\frac{5}{2}^+$	7.70 ± 1.50	8.20	6.61 (6.71)			
	$\frac{11}{2}^+$	$\frac{9}{2}^+$	$0.06^{+0.18}_{-0.06}$	0.20	··· (0.02)	0.20 ± 0.03	0.10	··· (0.21)
	$\frac{13}{2}^+$	$\frac{9}{2}^+$	5.0 ± 1.1	5.70	4.55 (4.46)			
	$\frac{11}{2}^+$	$\frac{13}{2}^+$	$3.0^{+9.0}_{-3.0}$	0.30	1.00 (0.84)	1.40 ± 0.20	1.80	··· (0.63)
^{31}P	$\frac{3}{2}^+$	$\frac{1}{2}^+$	4.00 ± 0.40	7.98	5.53	$(1.87 \pm 0.13) \times 10^{-2}$	2.63×10^{-2}	0.60×10^{-2}
	$\frac{5}{2}^+$	$\frac{1}{2}^+$	6.10 ± 0.30	7.69	5.50			
	$\frac{5}{2}^+$	$\frac{3}{2}^+$	<2.50	2.43	1.14	$<0.05 \times 10^{-2}$	0.12×10^{-2}	0.01×10^{-2}
	$\frac{7}{2}^+$	$\frac{3}{2}^+$	9.60 ± 1.60	10.63	7.85			
	$\frac{7}{2}^+$	$\frac{5}{2}^+$	<3.80	1.24	4.89	$<0.12 \times 10^{-2}$	3.37×10^{-2}	4.94×10^{-2}

TABLE III. The $M1$ transition strengths (in Weisskopf units) and $\log_{10} ft$ values of $\Delta T=1$ transitions are tabulated. The GT transitions in β^- decay of all the cases under consideration are from $T=T_z=\frac{3}{2}$ to $T=T_z=\frac{1}{2}$ states. Other notation is the same as in Table I.

				$M1$			$\log_{10} ft$	
Nucleus	J^π_i IAS	J^π_f	Expt	Present	SM	Expt	Present	SM
^{13}C	$\frac{3}{2}^-$	$\frac{1}{2}^-$	0.34 ± 0.09	0.29	0.55	4.01	4.16	3.88
	$\frac{3}{2}^-$	$\frac{3}{2}^-$	<0.86	0.31	···	4.53	4.77	4.78
	$\frac{3}{2}^-$	$\frac{5}{2}^-$				>4.7	5.04	5.23
^{19}F	$\frac{5}{2}^+$	$\frac{3}{2}^+$	0.56	0.30	0.25 (0.74)	4.45	4.75	4.60 (4.61)
	$\frac{5}{2}^+$	$\frac{5}{2}^+$	0.22	0.22	0.07 (0.26)	5.41	4.94	6.40 (5.53)
	$\frac{5}{2}^+$	$\frac{7}{2}^+$	2.60	0.45	0.11 (2.12)	3.54	4.68	4.20 (4.03)
	$\frac{3}{2}^+$	$\frac{1}{2}^+$	0.07	0.33	0.14 (0.43)	···	4.75	··· (5.08)
	$\frac{3}{2}^+$	$\frac{3}{2}^+$	0.12	0.48	0.16 (0.65)	···	4.55	··· (4.72)
	$\frac{3}{2}^+$	$\frac{5}{2}^+$	0.03	0.06	0.01 (0.04)	···	5.80	··· (7.81)
^{31}P	$\frac{1}{2}^+$	$\frac{1}{2}^+$	$(18.0 \pm 2.2) \times 10^{-2}$	20.3×10^{-2}	15.2×10^{-2}	5.56 ± 0.01	4.47	5.55
	$\frac{1}{2}^+$	$\frac{3}{2}^+$	$<1.6 \times 10^{-2}$	0.92×10^{-2}	1.10×10^{-2}	5.50 ± 0.10	5.25	5.50
	$\frac{3}{2}^+$	$\frac{1}{2}^+$	···	0.002×10^{-2}	1.12×10^{-2}			
	$\frac{3}{2}^+$	$\frac{3}{2}^+$	···	1.17×10^{-2}	0.37×10^{-2}			
	$\frac{3}{2}^+$	$\frac{5}{2}^+$	···	22.4×10^{-2}	11.9×10^{-2}			

are much larger than both the experimental values and the earlier SM calculations.[20] It can be observed from Table III that our $M1$ strengths consistently lie in between the two SM results of Refs. 16 and 20. We find that in some cases the logft value calculated from Eq. (9) using the total $B(M1)$ differs substantially from its actual calculated value. This is quite clear from the IAS $\frac{5}{2}^+$ to $\frac{7}{2}^+$ $M1$ transition strength and the corresponding logft value calculated in different models and in the actual experiment (Table III). Using the same quenching factor as discussed in connection with $\Delta T=0$ transitions (Table II), our calculated $M1$ transition strengths from the IAS $\frac{1}{2}^+$ to low-lying states of ^{31}P, and the corresponding logft values, are in good agreement with the experimental and SM results.[4,21] However, in the decay of the excited IAS $\frac{3}{2}^+$ to the low-lying states of ^{31}P, our results differ substantially from the SM results. This probably indicates that the excited IAS $\frac{3}{2}^+$ obtained from the $K=\frac{1}{2}$ band in ^{31}Si is not a good approximation to the actual state, because we find that there are other $K=\frac{1}{2}$ and $K=\frac{3}{2}$ bands energetically quite close to the one used in the present calculations.

4. CONCLUSIONS

The study of the decay of IAS provides an important tool for nuclear spectroscopy. In this paper we have analyzed recent experimental data on the IAS decay in ^{13}C, ^{19}F, and ^{31}P to their low-lying normal-parity states. This work was initiated by the success of the HF projection method in explaining the properties of the low-lying nuclear states. The present calculations were carried out by considering all the nucleons in the configuration space of the first four major oscillator shells using the NN interaction of Elliott *et al.*[5] In the case of ^{13}C, the computed magnetic moment and both $\Delta T=0$ and $\Delta T=1$ electromagnetic transitions together with corresponding logft values agree very well with the experimental observations. This good agreement in ^{13}C could be due to the availability of a large excitation configuration space. In the case of ^{19}F, the static moments, energy spectrum, and the $\Delta T=0$ electromagnetic transitions agree very well with the experimental data. In the $\Delta T=1$ $M1$ transitions, the agreement with the measured strengths for the decay of the IAS $\frac{5}{2}^+$ is better (excepting that to $\frac{7}{2}^+$) than that of the excited IAS $\frac{3}{2}^+$ in ^{19}F. It should be stated here that the results of the present calculations are just in between those of the two SM calculations.[16,20] The comparison of the calculated $M1$ transition strengths and the corresponding logft values for $\Delta T=1$ transitions shows that the contribution from the orbital part of $M1$ operator is not always negligible. In the case of ^{31}P, the calculated magnetic moment, $\Delta T=0$ $E2$ transition strengths, and $\Delta T=1$ $M1$ transition strengths for the decay of the IAS $\frac{1}{2}^+$ are in good agreement with the experimental data; the corresponding logft values for $\Delta T=1$ transitions are also in reasonable agreement. The present investigations lead us to conclude that the HF projection method successfully predicts both the $\Delta T=0$ and $\Delta T=1$ electromagnetic transition strengths and the logft values. The agreement for the $\Delta T=1$ electromagnetic transitions and ft values between the present and SM calculations is found to be nearly as good as was observed[9] in the case of $\Delta T=0$ transitions.

[1] J. D. Anderson and C. Wong, Phys. Rev. Letters 7, 250 (1961); 8, 442 (1962); J. D. Anderson, C. Wong, and J. W. McClure, Phys. Rev. 126, 2170 (1962); 129, 2718 (1963); J. D. Fox, C. F. Moore, and D. Robson, Phys. Rev. Letters 12, 198 (1964).

[2] J. D. Anderson, C. Wong, and J. W. McClure, Phys. Rev. 138, B615 (1965).

[3] S. S. Hanna, in *Isospin in Nuclear Physics*, edited by D. H. Wilkinson (North-Holland, Amsterdam, 1969).

[4] P. M. Endt, in *Nuclear Isospin*, edited by J. D. Anderson, S. D. Bloom, J. Cerny, and W. W. True (Academic, New York, 1969).

[5] J. P. Elliott, A. D. Jackson, H. A. Mavromatis, E. A. Sanderson, and B. Singh, Nucl. Phys. A121, 241 (1968).

[6] M. R. Gunye, J. Law, and R. K. Bhaduri, Nucl. Phys. A132, 225 (1969); M. R. Gunye, Phys. Letters 30B, 64 (1969); Nucl. Phys. A139, 686 (1969); A128, 457 (1969); M. R. Gunye and S. B. Khadkikar, Phys. Rev. Letters 24, 910 (1970).

[7] C. Mahaux and H. A. Weidenmuller, *Shell Model Approach to Nuclear Reactions* (North-Holland, Amsterdam, 1969), p. 280.

[8] L. A. Sliv and Yu. I. Kharitonov, Phys. Letters 16, 176 (1965); S. B. Khadkikar and C. S. Warke, Nucl. Phys. A130, 577 (1969).

[9] M. R. Gunye, Phys. Letters 27B, 136 (1968).

[10] E. Osnes and C. S. Warke, Nucl. Phys. A154, 331 (1970).

[11] M. R. Gunye and C. S. Warke, Phys. Rev. 156, 1087 (1967); 159, 885 (1967).

[12] C. S. Warke and M. R. Gunye, Phys. Rev. 155, 1084 (1967); I. Unna, *ibid.* 132, 2225 (1963); I. Kelson, Nucl. Phys. 89, 387 (1966).

[13] M. E. Rose, *Elementary Theory of Angular Momentum* (Wiley, New York, 1958).

[14] M. R. Gunye and C. S. Warke, Phys. Rev. 164, 1264 (1967).

[15] J. B. McGrory, Phys. Letters 31B, 339 (1970).

[16]A. Arima, M. Sakakura, and T. Sebe, Nucl. Phys. A170, 273 (1971).
[17]M. Bouten, P. Van Leuven, and H. Depuydt, Nucl. Phys. A94, 687 (1967); M. R. Gunye and S. B. Khadkikar, to be published.
[18]S. Cohen and D. Kurath, Nucl. Phys. 73, 1 (1965).
[19]C. L. Cocke, J. C. Adloff, and P. Chevallier, Phys. Rev. 176, 1120 (1968); F. S. Dietrich, M. Suffert, A. V. Nero, and S. S. Hanna, Phys. Rev. 168, 1169 (1968).
[20]J. H. Aitken, A. E. Litherland, W. R. Dixon, and R. S. Storey, Phys. Letters 30B, 473 (1969). K. P. Jackson, K. B. Ram, P. G. Lawson, N. G. Chapman, and K. W. Allen, *ibid.* 30B, 162 (1969); D. D. Tolbert, Ph.D. thesis, University of Kansas, 1968 (unpublished).
[21]P. M. W. Glaudemans, A. E. L. Dieperink, R. J. Keddy, and P. M. Endt, Phys. Letters 28B, 645 (1969).
[22]A. R. Poletti, E. K. Warburton, and D. Kurath, Phys. Rev. 155, 1096 (1967).

PHYSICAL REVIEW C VOLUME 5, NUMBER 6 JUNE 1972

Photon Spectra from Radiative Absorption of Pions in Nuclei*

J. A. Bistirlich, K. M. Crowe, A. S. L. Parsons,† P. Skarek,‡ and P. Truöl§
Lawrence Berkeley Laboratory, University of California, Berkeley, California 94720
(Received 27 December 1971)

The photon spectra following capture of stopped pions in ^{4}He, ^{12}C, ^{16}O, ^{24}Mg, and ^{40}Ca have been measured for photon energies between 50 and 160 MeV. A pair spectrometer was used and a resolution of 2.0 MeV (full width at half maximum) was achieved. On the basis of several thousand events for each spectrum, we observe collective excitation in the residual nucleus for capture on ^{4}He, ^{12}C, and ^{16}O. Such excitation is predicted theoretically, and in some cases the detailed comparison with the data is good. For ^{24}Mg and ^{40}Ca, no significant structure is seen. In addition, the transition rates to particle-stable states in ^{16}O and ^{12}C have been measured. A continuum background consistent with a direct-reaction mechanism is also observed for all the elements studied except for ^{4}He. Results for the pion-capture rates in CH_2 and H_2O are given.

I. INTRODUCTION

Using a pair spectrometer we have measured the photon energy spectrum between 50 and 160 MeV, arising from the radiative capture of stopped pions in various nuclei: ^{4}He, ^{12}C, ^{16}O, ^{24}Mg, and ^{40}Ca. Although data from ^{4}He and ^{12}C have already been published,[1,2] we present them with the new data for completeness. Discussion of these two elements will be confined mainly to new information.

In this section we discuss the theoretical and experimental background to the radiative capture process. In Sec. II we describe the experimental technique; and in Sec. III we discuss our results for each element, together with earlier experimental work for that element and relevant theoretical predictions.

The process under study, expressed generally, is

$$\pi^- + N(A, Z) \rightarrow N^*(A, Z-1) + \gamma . \qquad (1)$$

For the lighest nuclei, the pion will be captured mainly from a $1s$ Bohr orbit; as the mass of the nucleus increases, capture from $2p$ and higher orbits predominates (for example, about 80% of pions are captured from $2p$ orbits in ^{12}C). Radiative capture is typically ~2% of the total capture rate. Much of the interest in this process derives from its close similarity with negative-muon capture,

$$\mu^- + N(A, Z) \rightarrow N^*(A, Z-1) + \nu_\mu , \qquad (2)$$

in which the capture is always from $1s$ orbits and accounts for essentially the whole rate. The analogy has been extensively discussed in theoretical terms in the recent literature; only the more prominent features of it will be mentioned here.

The most obvious analogy between reactions (1) and (2) arises from the closeness of the masses of the participating particles, so that the momentum transfers are of the same order $-0.92m_\pi^2$ for (1) and $0.52m_\pi^2$ for (2). A more subtle and far-reaching analogy comes from the fact that the matrix element for pion capture, reaction (1), leading to a particular final state can be expressed in terms of the same axial-vector and pseudoscalar nuclear form factors (f_A and f_p) as appear in the muon-capture matrix element to the same final state: Muon capture has additional vector terms. This equality has been derived using both the impulse approximation and partially conserved axial-vector current (PCAC).[3] However, the impulse approximation has been compared with the PCAC